

## LOCATING THE QCD CRITICAL POINT IN THE PHASE DIAGRAM

N. G. Antoniou, F. K. Diakonov and A. S. Kapoyannis  
*Department of Physics, University of Athens, 15771 Athens, Greece*

Presented at the X International Workshop on Multiparticle Production  
“Correlations and Fluctuations on QCD”,  
8-15 June 2002, Istron Bay, Ag. Nikolaos, Crete, GREECE

### Abstract

It is shown that the hadronic matter formed at high temperatures, according to the prescription of the statistical bootstrap principle, develops a critical point at nonzero baryon chemical potential, associated with the end point of a first-order, quark-hadron phase-transition line. The location of the critical point is evaluated as a function of the MIT bag constant.

PACS numbers: 25.75.-q, 12.40.Ee, 12.38.Mh, 05.70.Ce

Keywords: Statistical Bootstrap Model

## 1 Introduction

Quantum Chromodynamics is unquestionably the microscopic theory of strong interactions and offers an accurate description of quark-gluon matter. The formation of hadronic matter is still an open problem in the context of QCD. This theory predicts however the existence of a critical point at non zero baryon chemical potential, which is the end point of a quark-hadron critical line of first order [1]. This singularity is associated with the formation of hadronic matter at high temperatures and its location in the QCD phase diagram is of primary importance.

On the other hand the hadronic side of matter can be treated as a thermally and chemically equilibrated gas. The inclusion of *interactions* among hadrons is crucial in order to reveal the possibility of a phase transition. A model that allows for the thermodynamical description of interacting hadrons is the Statistical Bootstrap Model (SBM), which was first developed by Hagedorn [2-5]. In what follows we investigate the possibility of the formation of a critical point within the framework of the statistical bootstrap hypothesis.

## 2 The hadronic matter

The SBM is based on the hypothesis that the strong interactions can be simulated by the presence of hadronic clusters. In the context of SBM the strongly interacting hadron gas is replaced by a non-interacting infinite-component cluster gas. The hadronic states of clusters are listed in a mass spectrum  $\tilde{\rho}$ , so that  $\tilde{\rho}dm$  represents the number of hadronic states in the mass interval  $\{m, m + dm\}$ . The mass spectrum can be evaluated if the clusters, as well as, their constituents are treated on the same footing by introducing an integral *bootstrap* equation (BE). In the bootstrap logic clusters are composed of clusters described by the same mass spectrum. This scheme proceeds until clusters are reached that their constituents cannot be divided further. These constituents are the *input* hadrons and the known hadronic particles belong to

this category. The BE leads to the adoption of an asymptotic mass spectrum of the form [7]

$$\tilde{\rho}(m^2, \{\lambda\}) \xrightarrow{m \rightarrow \infty} 2C(\{\lambda\})m^{-\alpha} \exp[m\beta^*(\{\lambda\})] . \quad (1)$$

The underlying feature of SBM is that the mass spectrum rises *exponentially*, as  $m$  tends to infinity.  $\beta^*$  is the inverse maximum temperature allowed for hadronic matter and depends on the existing fugacities  $\{\lambda\}$ .  $\alpha$  is an exponent which can be adjusted to different values allowing for different versions of the model.

The manipulation of the bootstrap equation can be significantly simplified through suitable Laplace transformations. The Laplace transformed mass spectrum leads to the introduction of the quantity  $G(\beta, \{\lambda\})$ . The same transformation can be carried out to the input term of SBM, leading to the quantity  $\varphi(\beta, \{\lambda\})$ . Then the BE can be expressed as

$$\varphi(\beta, \{\lambda\}) = 2G(\beta, \{\lambda\}) - \exp[G(\beta, \{\lambda\})] + 1 . \quad (2)$$

The above BE exhibits a singularity at

$$\varphi(\beta, \{\lambda\}) = \ln 4 - 1 . \quad (3)$$

The last equation imposes a constraint among the thermodynamic variables which represent the *boundaries* of the hadronic phase. Hadronic matter can exist in all states represented by variables that lead to a real solution of the BE or equivalently in all states for which temperatures and fugacities lead to

$$\varphi(\beta, \{\lambda\}) \leq \ln 4 - 1 . \quad (4)$$

In the general form of SBM the following four improvements can be made which allow for a better description of hadronic matter:

1) The inclusion of all the known hadrons with masses up to 2400 MeV in the input term of the BE and also inclusion of strange hadrons. This leads to the introduction of the strangeness fugacity  $\lambda_s$  in the set of fugacities [6,7]. Another fugacity which

is useful for the analysis of the experimental data in heavy ion collisions is  $\gamma_s$ . This fugacity allows for partial strangeness equilibrium and can also be included in the set of fugacities of SBM [8].

2) Different fugacities can be introduced for  $u$  and  $d$  quarks. In this way the thermodynamic description of systems which are not isospin symmetric becomes possible. Such systems can emerge from the collision of nuclei with different number of protons and neutrons [9].

3) The choice of the exponent  $\alpha$  in (1) has important consequences, since every choice leads to a different physical behaviour of the system. The usual SBM choice was  $\alpha = 2$ , but more advantageous is the choice  $\alpha = 4$ . With this choice a better physical behaviour is achieved as the system approaches the hadronic boundaries. Quantities like pressure, baryon density and energy density, even for point-like particles, no longer tend to infinity as the system tends to the bootstrap singularity. It also allows for the bootstrap singularity to be reached in the thermodynamic limit [10], a necessity imposed by the Lee-Yang theory. Another point in favour of the choice  $\alpha = 4$  comes from the extension of SBM to include strangeness [6,7]. The strange chemical potential equals zero in the quark-gluon phase. With this particular choice of  $\alpha$ ,  $\mu_s$  acquires smaller positive values as the hadronic boundaries are approached. After choosing  $\alpha = 4$  the partition function can be written down and for point-like particles it assumes the form

$$\ln Z_{p\text{ SBM}}(V, \beta, \{\lambda\}) = \frac{4BV}{\beta^3} \int_{\beta}^{\infty} x^3 G(x, \{\lambda\}) dx \equiv V f_{SBM}(\beta, \{\lambda\}), \quad (5)$$

where  $B$  is the energy density of the vacuum (bag constant) and it is the only free parameter of SBM which is left after fixing  $\alpha = 4$  [6,7].

4) The contributions due to the finite size of hadrons, accounting for the repulsive interaction among hadrons, can be introduced via a Van der Waals treatment of the volume. The negative contributions to the volume can be avoided if the following

grand canonical pressure partition function is used

$$\pi(\xi, \beta, \{\lambda\}) = \frac{1}{\xi - f(\beta + \xi/4B, \{\lambda\})}, \quad (6)$$

where  $\xi$  is the Laplace conjugate variable of the volume. All values of  $\xi$  are allowed if Gaussian regularization is performed [11]. The value  $\xi = 0$  corresponds to a system without external forces [10,11] and it will be used throughout our calculations. With the use of (6) and the SBM point particle partition function (5) one obtains

$$\nu_{HG}(\xi, \beta, \{\lambda\}) = \lambda \frac{\frac{\partial f(\beta + \xi/4B, \{\lambda\})}{\partial \lambda}}{1 - \frac{1}{4B} \frac{\partial f(\beta + \xi/4B, \{\lambda\})}{\partial \beta}}, \quad (7)$$

where  $\lambda$  is the fugacity corresponding to the particular density, and

$$P_{HG}(\xi, \beta, \{\lambda\}) = \frac{1}{\beta} \frac{f(\beta + \xi/4B, \{\lambda\}) - \frac{\xi}{4B} \frac{\partial f(\beta + \xi/4B, \{\lambda\})}{\partial \beta}}{1 - \frac{1}{4B} \frac{\partial f(\beta + \xi/4B, \{\lambda\})}{\partial \beta}}. \quad (8)$$

The dependence of the pressure on the volume can be recovered if for a given set of parameters  $\xi, \beta, \{\lambda\}$  the density  $\nu_b$  of the conserved baryon number  $\langle b \rangle$  is calculated. Then the volume would be retrieved through the relation

$$\langle V \rangle = \frac{\langle b \rangle}{\nu_b}. \quad (9)$$

By using the SBM with all the above improvements the possibility of a phase transition of hadronic matter can be traced. The study of the pressure-volume isotherm curve is then necessary. When this curve is calculated one important feature of SBM is revealed. This curve has a part (near the boundaries of the hadronic domain) where pressure decreases while volume decreases also (see Fig.1). This behaviour is due to the formation of bigger and bigger clusters as the system tends to its boundaries. Such a behaviour is a signal of a *first order phase transition* which in turn is connected with the need of a *Maxwell construction*.

If on the contrary the interaction included in SBM is not used then no such behaviour is exhibited. This can be verified if the Ideal Hadron Gas model is used.

Then for this model the equation that corresponds to Eq. (5) is

$$f_{p\ IHG}(\beta, \{\lambda\}) \equiv \frac{\ln Z_{p\ IHG}(V, \beta, \{\lambda\})}{V} = \frac{1}{2\pi^2\beta} \sum_a [\lambda_a(\{\lambda\}) + \lambda_a(\{\lambda\})^{-1}] \sum_i g_{ai} m_{ai} K_2(\beta m_{ai}), \quad (10)$$

where  $g_{ai}$  are degeneracy factors due to spin and isospin and  $a$  runs to all hadronic families. This function can be used in eq. (6) to calculate the Ideal Hadron Gas (IHG) pressure partition function in order to include Van der Waals volume corrections. The result is that the pressure is always found to increase as volume decreases, for constant temperature, allowing for no possibility of a phase transition.

The comparison of SBM with the IHG (with volume corrections) is displayed in Figure 1, where  $\nu_0$  is the normal nuclear density  $\nu_0 = 0.14\ fm^{-3}$ . In both cases (SBM or IHG) the constraints  $\langle S \rangle = 0$  (zero strangeness) and  $\langle b \rangle = 2 \langle Q \rangle$  (isospin symmetric system, i.e. the net number of  $u$  and  $d$  quarks are equal) have been imposed. Also strangeness is fully equilibrated which accounts to setting  $\gamma_s = 1$ .

### 3 The quark-gluon matter

We may now proceed to the thermodynamical description of the quark-gluon phase. The grand canonical partition function of a system containing only  $u$  and  $d$  massless quarks and gluons is [13]

$$\begin{aligned} \ln Z_{QGP}(V, \beta, \lambda_q) = & \underbrace{\frac{gV}{6\pi^2}\beta^{-3} \left[ \left(1 - \frac{2a_s}{\pi}\right) \left(\frac{1}{4}\ln^4 \lambda_q + \frac{\pi^2}{2}\ln^2 \lambda_q\right) + \left(1 - \frac{50a_s}{21\pi}\right) \frac{7\pi^4}{60} \right]}_{\text{quark term}} \\ & + \underbrace{V \frac{8\pi^2}{45}\beta^{-3} \left(1 - \frac{15a_s}{4\pi}\right)}_{\text{gluon term}} - \underbrace{\beta BV}_{\text{vacuum term}}. \end{aligned} \quad (11)$$

This partition function is calculated to first order in the QCD running coupling constant  $a_s$ . The fugacity  $\lambda_q$  is related to both  $u$  and  $d$  quarks.  $B$  is again the MIT bag constant and  $g$  equals to the product of spin states, colours and flavours available in

the system,  $g = N_s N_c N_f = 12$ . Using this partition function the QGP baryon density and pressure can be calculated through the relations

$$\nu_{b\ QGP}(\beta, \lambda_q) = \frac{2}{\pi^2} \beta^{-3} \left(1 - \frac{2a_s}{\pi}\right) \left(\frac{1}{3} \ln^3 \lambda_q + \frac{\pi^2}{3} \ln \lambda_q\right) \quad (12)$$

$$P_{QGP}(\beta, \lambda_q) = \frac{2}{\pi^2} \beta^{-4} \left[ \left(1 - \frac{2a_s}{\pi}\right) \left(\frac{1}{4} \ln^4 \lambda_q + \frac{\pi^2}{2} \ln^2 \lambda_q\right) + \left(1 - \frac{50a_s}{21\pi}\right) \frac{7\pi^4}{60} \right] + \frac{8\pi^2}{45} \beta^{-4} \left(1 - \frac{15a_s}{4\pi}\right) - B. \quad (13)$$

If the strange quarks are also included, the quarks assume their current masses and  $a_s = 0$ , then the following partition function can be used.

$$\begin{aligned} \ln Z_{QGP}(V, \beta, \lambda_u, \lambda_d) = & \underbrace{\frac{N_s N_c V}{6\pi^2} \beta \sum_i \int_0^\infty \frac{p^4}{\sqrt{p^2 + m_i^2}} \frac{1}{e^{\beta\sqrt{p^2 + m_i^2}} \lambda_i^{-1} + 1} dp}_{\text{quark term}} \\ & + \underbrace{V \frac{8\pi^2}{45} \beta^{-3}}_{\text{gluon term}} - \underbrace{\beta B V}_{\text{vacuum term}}. \end{aligned} \quad (14)$$

The index  $i$  runs to all quarks and antiquarks. The current masses are taken  $m_u = 5.6$  MeV,  $m_d = 9.9$  MeV and  $m_s = 199$  MeV [14]. The fugacities are  $\lambda_{\bar{u}} = \lambda_u^{-1}$ ,  $\lambda_{\bar{d}} = \lambda_d^{-1}$  and  $\lambda_{\bar{s}} = \lambda_s^{-1} = 1$  (since strangeness is set to zero). The baryon density is then

$$\nu_{b\ QGP}(\beta, \lambda_u, \lambda_d) = \frac{N_s N_c}{2\pi^2} \sum_i N_i \int_0^\infty \frac{p^2}{e^{\beta\sqrt{p^2 + m_i^2}} \lambda_i^{-1} + 1} dp, \quad (15)$$

where  $i$  includes only  $u$ ,  $\bar{u}$ ,  $d$  and  $\bar{d}$  quarks and  $N_i = 1$  for  $u$  and  $d$  quarks and  $N_i = -1$  for  $\bar{u}$  and  $\bar{d}$  quarks. The pressure is

$$P_{QGP}(\beta, \lambda_u, \lambda_d) = \frac{1}{\beta} \frac{\ln Z_{QGP}(V, \beta, \lambda_u, \lambda_d)}{V}. \quad (16)$$

In order to study the effect of the inclusion of strange quarks we can use the partition function (11) and add the part of the quark term of (14) which corresponds to the strange quarks.

#### 4 Matching the two phases

After completing a thermodynamic description for the hadronic and for the quark-gluon phase we can trace whether a phase transition can occur between the two phases. Similar situations have been studied in [10,12,13], but here, apart from the use of the SBM incorporating all four improvements, we shall focus our calculations to the location of the critical point. So no value of  $B$  or  $a_s$  will be selected a-priori.

If  $a_s$  and  $\xi$  are fixed, then the only free parameter left would be the MIT bag constant  $B$ . If a value of  $B$  is chosen, also, the pressure-volume isotherms of Hadron Gas and QGP can be calculated for a specific temperature. Then at the point where the two isotherms meet would correspond equal volumes and equal pressures for the two phases. But assuming that the baryon number is a conserved quantity to both phases, the equality of volumes would lead to the equality of baryon densities.

When performing calculations about the location of the point where the two phases meet, with fixed MIT bag constant, what is found is that at a low temperature the QGP and SBM pressure-volume isotherms meet at a point where the Hadron Gas pressure is *decreasing* while volume *decreases*. This is reminiscent of the need of a Maxwell construction. So at that point the phase transition between Hadron Gas and QGP must be of *first order*. As the temperature rises, a certain temperature is found for which the QGP isotherm meets the SBM isotherm at a point which corresponds to the maximum Hadron Gas pressure for this temperature. So no Maxwell construction is needed. It is important to notice that this point is located at *finite volume* or *finite baryon density* and it can be associated with the QCD critical point. Then, as temperature continues to rise, the QGP isotherms meet the SBM isotherms at points with even greater volume. Again no Maxwell construction is needed and this region belongs to the *crossover* area.

These situations can be depicted in Figure 2, where all curves have been calculated for  $B^{1/4} = 210$  MeV. The dotted curved lines correspond to SBM, while the almost straight dotted lines correspond to QGP. For the calculations three quark flavours



have been used with their corresponding current masses and  $a_s = 0$ . The thick lines are the resulting pressure-volume curves for the Hadron Gas-QGP system. A Maxwell construction is needed for the low temperature isotherm. This is depicted by the horizontal line which is drawn so that the two shaded surfaces are equal and represents the final pressure-volume curve after the completion of the Maxwell construction. In the same figure the isotherm that leads the pressure curves of the two phases to meet at the maximum hadron gas pressure, forming a critical point, is drawn, also. Finally for higher temperatures the two curves meet at a point so that the resulting pressure curve is always increasing as volume decreases, without the need of a Maxwell construction (crossover area).

A more detailed figure of the previous one is Figure 3, where more curves that need Maxwell construction can be displayed. The coexistence region of the two phases are represented by the horizontal Maxwell constructed curves. The slashed line represents the boundaries of the Maxwell construction and so the boundaries of the coexistence region.

## 5 Locating the Critical Point

To locate the critical point with the choice (14) for the QGP partition function, for a given  $B$ , one has to determine the parameters  $(\beta, \lambda_u, \lambda_d, \lambda_s, \lambda'_u, \lambda'_d)$ , which solve the following set of equations.

$$\nu_{b\ SBM}(\beta, \lambda_u, \lambda_d, \lambda_s) = \nu_{b\ QGP}(\beta, \lambda'_u, \lambda'_d) \quad (17a)$$

$$P_{SBM}(\beta, \lambda_u, \lambda_d, \lambda_s) = P_{QGP}(\beta, \lambda'_u, \lambda'_d) \quad (17b)$$

$$\frac{\partial P_{SBM}(\beta, \lambda_u, \lambda_d, \lambda_s)}{\partial \lambda_u} = 0 \quad (17c)$$

$$\langle S(\beta, \lambda_u, \lambda_d, \lambda_s) \rangle_{SBM} = 0 \quad (17d)$$

$$\langle b(\beta, \lambda_u, \lambda_d, \lambda_s) \rangle_{SBM} - 2 \langle Q(\beta, \lambda_u, \lambda_d, \lambda_s) \rangle_{SBM} = 0 \quad (17e)$$

$$\langle b(\beta, \lambda'_u, \lambda'_d) \rangle_{QGP} - 2 \langle Q(\beta, \lambda'_u, \lambda'_d) \rangle_{QGP} = 0 \quad (17f)$$

Eq. (17c) is equivalent to  $P_{SBM} = P_{SBM \max}$ , when all the rest of the equations are valid. Eq. (17d) imposes zero strangeness to HG phase. Eqs. (17e) and (17f) account for isospin symmetry in the HG and QGP phase, respectively. Also we have set  $\gamma_s = 1$  assuming full strangeness equilibrium.

With the choice (11) for the QGP partition function only the equations (17a)-(17e) have to be solved, since only one fugacity  $\lambda_q = \lambda'_u = \lambda'_d$  is available in the QGP phase.

The calculations for the position of the critical point for different values of  $B$  are presented in Figures 4-6. The range of values of  $B^{1/4} = (145 - 235)$  MeV [14,15] has been used for these calculations. In Figure 4 we depict the critical temperature as a function of the critical baryon density. The dotted curves correspond to the QGP partition function with massless  $u$  and  $d$  quarks, without strange quarks and for different values of  $a_s$ . The thick solid curve corresponds to the QGP partition function with massive  $u$ ,  $d$  and  $s$  quarks and  $a_s = 0$ . The slashed curve corresponds to the QGP partition function with massless  $u$ ,  $d$ , massive  $s$  quarks and  $a_s = 0.1$ .

Figure 5 presents the connection of the MIT bag constant with the baryon density of the critical point, divided by the normal nuclear density.

In Figure 6 the critical temperature is plotted versus the critical baryon chemical potential. The code of lines are as in Figure 4. In this graph the lines representing the bootstrap singularity, that is the boundaries of the maximum space allowed to the hadronic phase, for the maximum and minimum values of  $B$ , are also depicted (slashed-dotted curves). The filled circles represent positions of critical point for the different choices of the QGP partition functions for these maximum and minimum values of  $B$ . As it can be seen the critical point is placed within the hadronic phase, close to the bootstrap singularity. Every modification made to external parameters drives the critical point in parallel to the bootstrap singularity line.

Typical values for the position of the critical point are listed in Table 1.

## 6 Concluding Remarks

From our study we may conclude that, as  $B$  increases, the critical point moves to higher baryon density, smaller baryon chemical potential and higher temperature until a certain value of  $B$  is reached. If  $B$  is increased further, then the critical point moves quickly to zero baryon density and zero baryon chemical potential, while temperature keeps increasing slowly.

The inclusion of strange quarks always moves the critical point to higher baryon density and higher baryon chemical potential (for fixed values of  $B$  and  $a_s$ ).

As  $a_s$  is increased (at the same QGP partition function), the critical point moves to smaller baryon density, smaller baryon chemical potential and higher temperature, while the move of the critical point towards zero chemical potential takes place at smaller values of  $B$ .

From the last two remarks we can infer that the calculation with massive quarks and  $a_s = 0$  represents the *higher* baryon density, *higher* baryon chemical potential and *smaller* temperature (for a given  $B$ ) that the critical point can acquire. So this particular QGP partition function can give us an *upper* limit for the position of the critical point in baryon density or baryon chemical potential.

From Figure 6 it is evident that the critical point is positioned near the bootstrap singularity curve. So this curve can represent, to a good approximation, the first-order transition line between hadron and quark-gluon phase.

From Table 1 we observe that in the minimal, two flavour version of the quark-gluon description ( $a_s = 0$ ) and in the chiral limit ( $m_u = m_d = 0$ ), where the critical point becomes tricritical, the location of the singularity may come close to the freeze-out area of the SPS experiments (typically:  $T_c \approx 171$  MeV,  $\mu_c \approx 300$  MeV). On the contrary, the Lattice QCD solution [16] with unphysically large values of the quark masses  $m_u, m_d$  drives the critical baryon chemical potential to higher values ( $T_c \approx 160$  MeV,  $\mu_c \approx 725$  MeV). In order to bridge this discrepancy one needs an improvement in both approaches. In the bootstrap approach a realistic partition function of the

quark-gluon matter is needed, based not on perturbation theory but on the knowledge of the quark-gluon pressure on the lattice for nonzero chemical potential. At present, there exist lattice results for the pressure only for  $\mu = 0$  [17]. In the lattice search for the critical point on the other hand the solution for small quark masses (chiral limit) is needed before any quantitative comparison, both with the bootstrap solution and the location of the freeze-out area in heavy-ion collisions, could be made.

## References

- [1] F. Wilczek, hep-ph/0003183; J. Berges, K. Rajagopal, Nucl. Phys. B538 (1999) 115
- [2] Hagedorn R 1965 Suppl. Nuovo Cimento III 147
- [3] Hagedorn R and Ranft J 1968 Suppl. Nuovo Cimento VI 169; Hagedorn R 1968 Suppl. Nuovo Cimento VI 311
- [4] Hagedorn R 1968 Nuovo Cimento LVI A 1027
- [5] Hagedorn R and Rafelski J 1980 Phys. Lett. 97B 136
- [6] Kapoyannis A S, Ktorides C N and Panagiotou A D 1997 J. Phys. G 23 1921
- [7] Kapoyannis A S, Ktorides C N and Panagiotou A D 1998 Phys. Rev. D 58 034009
- [8] Kapoyannis A S, Ktorides C N and Panagiotou A D 1998 Phys. Rev. C 58 2879
- [9] Kapoyannis A S, Ktorides C N and Panagiotou A D 2000 Eur. Phys. J. C 14 299
- [10] Letessier J and Tounsi A 1988 Nuovo Cimento 99A 521
- [11] Hagedorn R 1983 Z. Phys. C 17 265
- [12] Fiore R, Hagedorn R and d' Isep F 1985 Nuovo Cimento 88A 301

- [13] Rafelski J and Hagedorn R: From hadron gas to quark matter II. In: Statistical mechanics of quarks and hadrons, H. Satz (Ed.), Amsterdam: North Holland 1981
- [14] Cheuk-Yin Wong: Introduction to High-Energy Heavy-Ion Collisions, World Scientific Publishing 1994
- [15] Haxton W C and Heller L 1980 Phys. Rev. D 22 1198; Hasenfratz P, Horgan R R, Kuti J and Richard J M 1981 Phys. Lett. 95 B 199
- [16] Fodor Z and Katz S D, hep-lat/0106002
- [17] Karsch F, Laermann E and Peikert A 2000 Phys. Lett. 478 B 447

### Figure Captions

**Figure 1** Isotherm pressure-volume curve for SBM and IHG (both with Van der Waals volume corrections using the pressure ensemble).  $B$  is constant.

**Figure 2** Three isotherm pressure-volume curves for Hadron Gas (using SBM) and QGP phase (using partition function including  $u$ ,  $d$  and  $s$  quarks at their current masses and  $a_s = 0$ ). The low temperature isotherm needs Maxwell construction, the middle temperature isotherm corresponds to critical point and the high temperature isotherm corresponds to crossover.  $B$  is constant.

**Figure 3** A similar case as in Figure 2. The boundaries of Maxwell construction are displayed with the slashed line.

**Figure 4** The baryon density at the critical point versus the critical temperature for different values of  $B$  and for different types of the QGP partition function.

**Figure 5** The critical temperature as a function of the MIT bag constant for different types of the QGP partition function.

**Figure 6** Critical temperature versus critical baryon chemical potential for different values of  $B$  and for different types of QGP partition functions. The bootstrap singularity lines for maximum and minimum values of  $B$ , as well as, the critical points corresponding to these values (filled circles) are also displayed.

| $B^{1/4}$ (MeV)  | $\nu_{b\ cr.p.}$ ( $\text{fm}^{-3}$ ) | $T_c$ (MeV) | $\mu_c$ (MeV) |
|--|---------------------------------------|-------------|---------------|
| $a_s = 0, m_u = m_d = 0, s\text{-quarks not included}$                         |                                       |             |               |
| 235  | 0.2158                                | 171.2       | 299.4         |
| 180  | 0.1361                                | 127.9       | 544.5         |
| 145  | 0.0690                                | 102.6       | 623.4         |
| $a_s = 0, m_u = 5.6\ \text{MeV}, m_d = 9.9\ \text{MeV}, m_s = 199\ \text{MeV}$ |                                       |             |               |
| 235  | 0.3110                                | 159.1       | 451.1         |
| 180  | 0.1489                                | 121.2       | 598.6         |
| 145  | 0.0721                                | 98.4        | 651.9         |

Table 1.

### Table Caption

**Table 1** Some values for the position of the critical point for different values of  $B$  and different QGP partition functions.

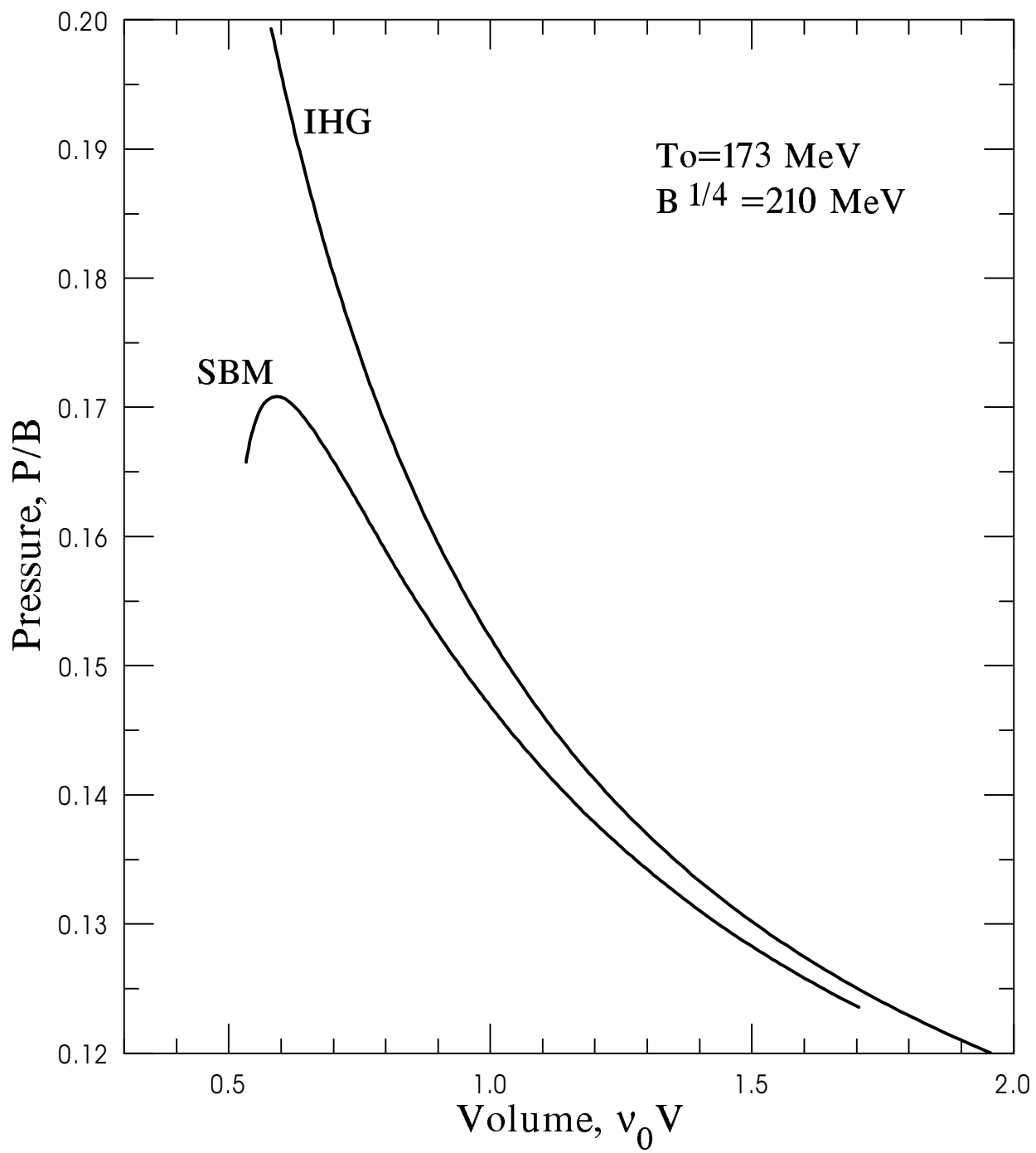


Fig. 1

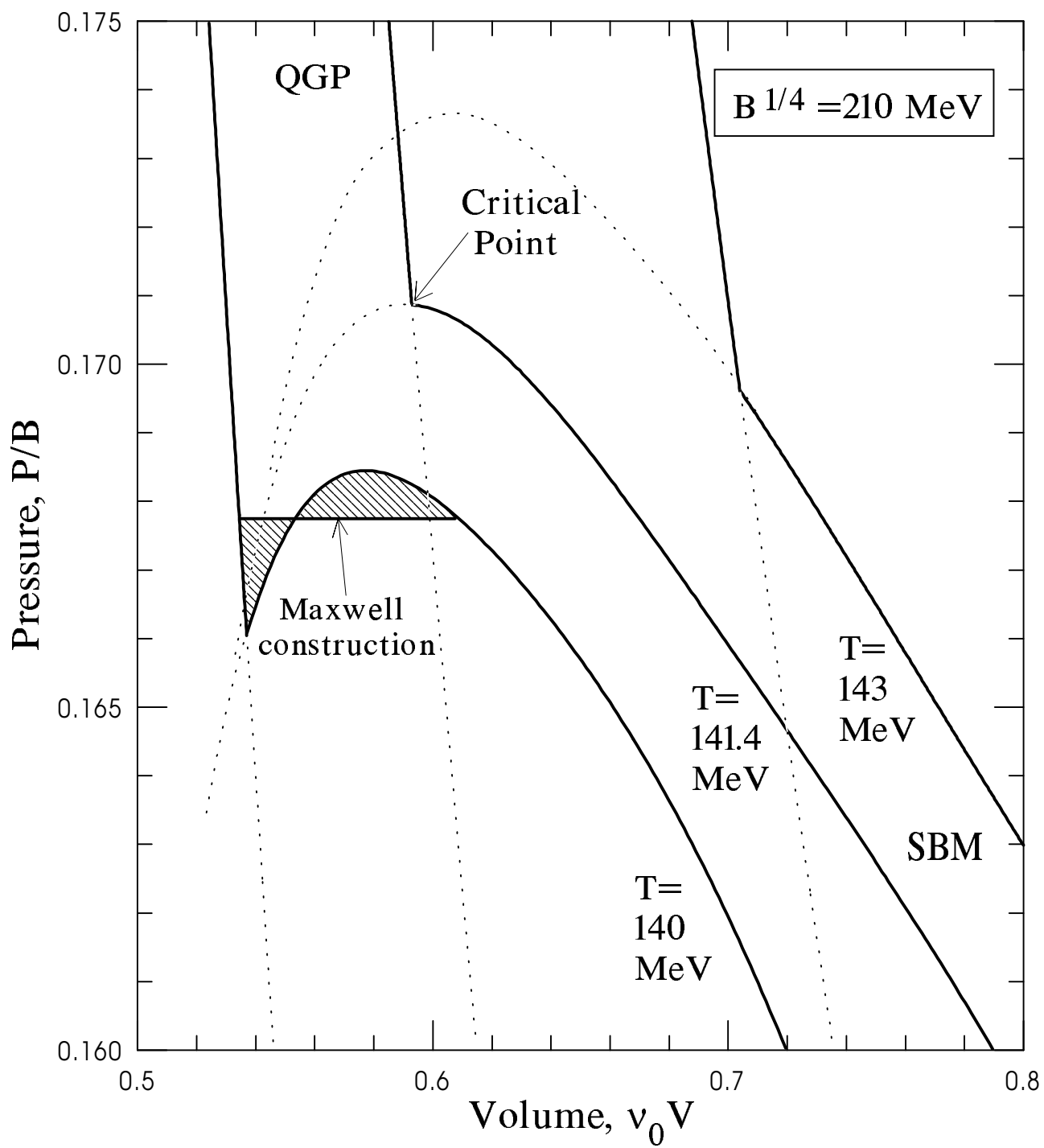


Fig. 2



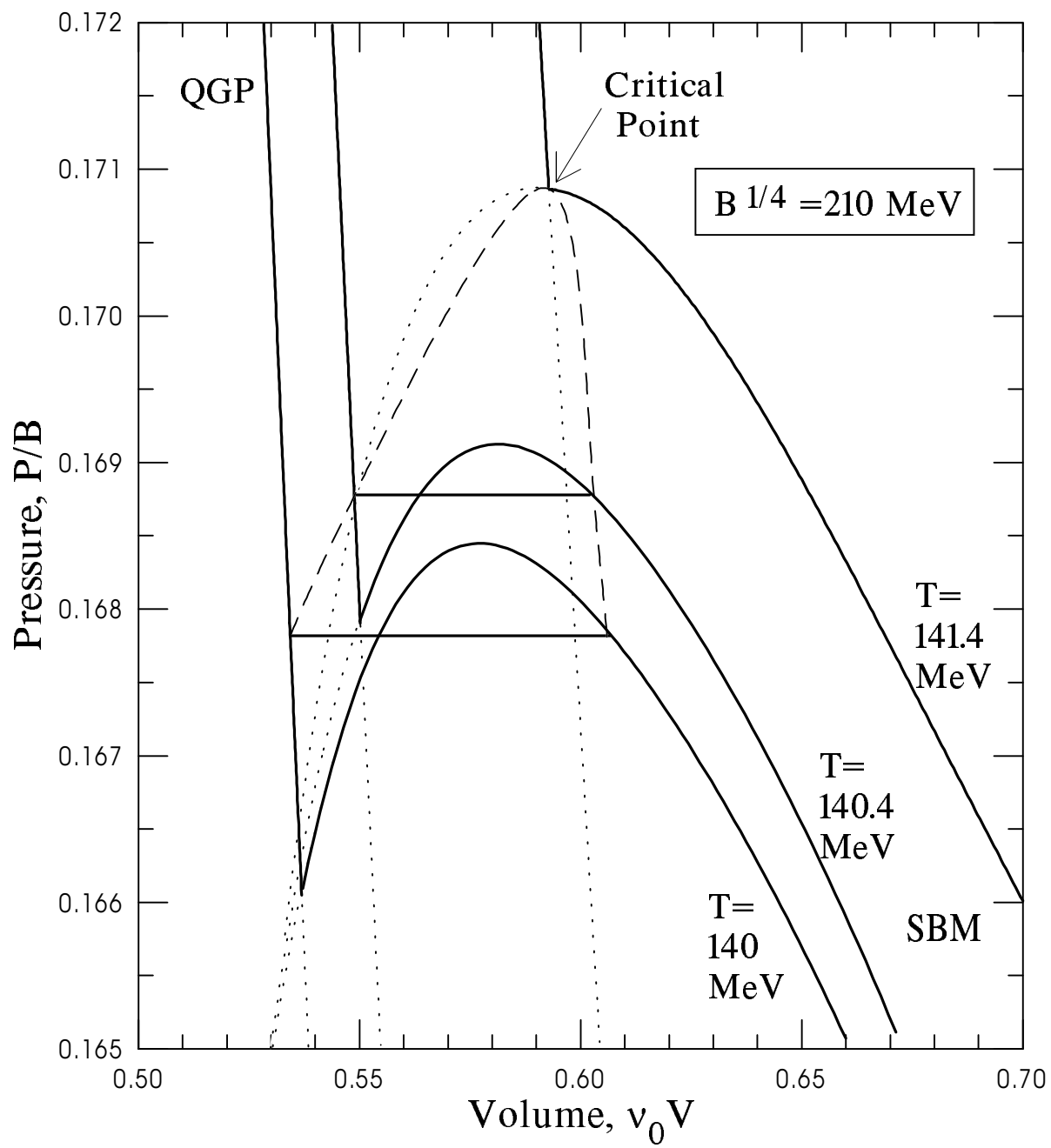


Fig. 3

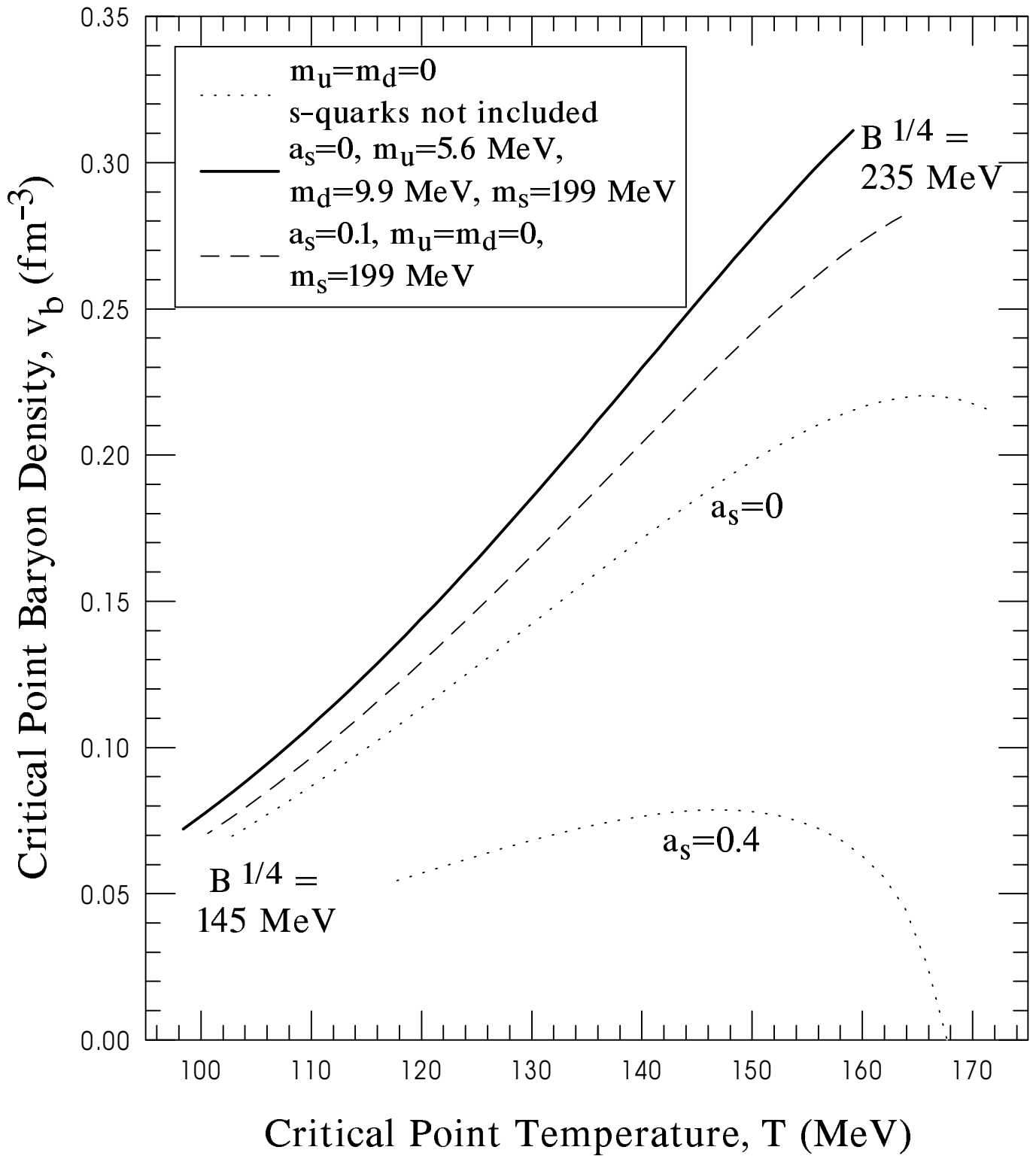


Fig. 4

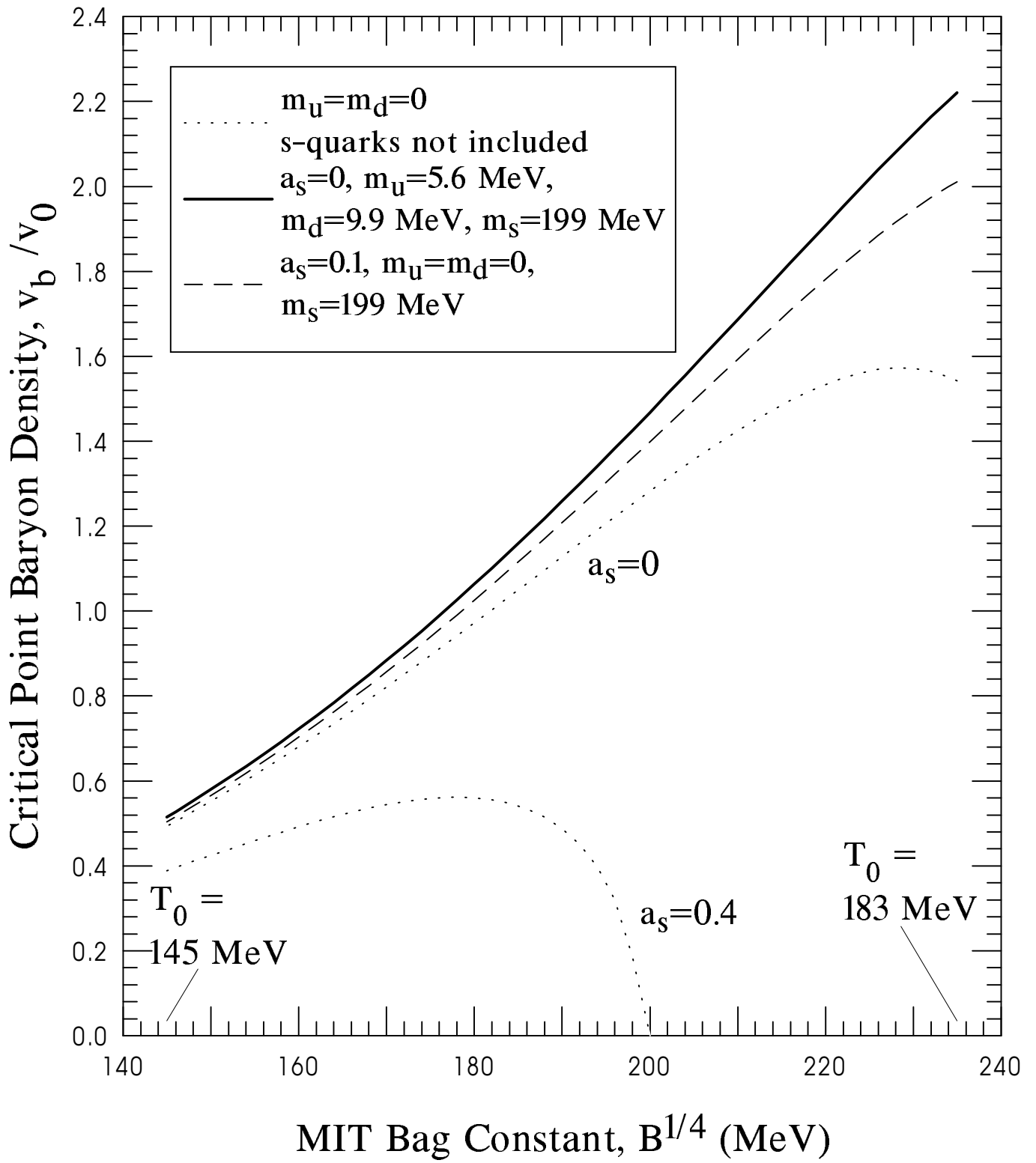


Fig. 5

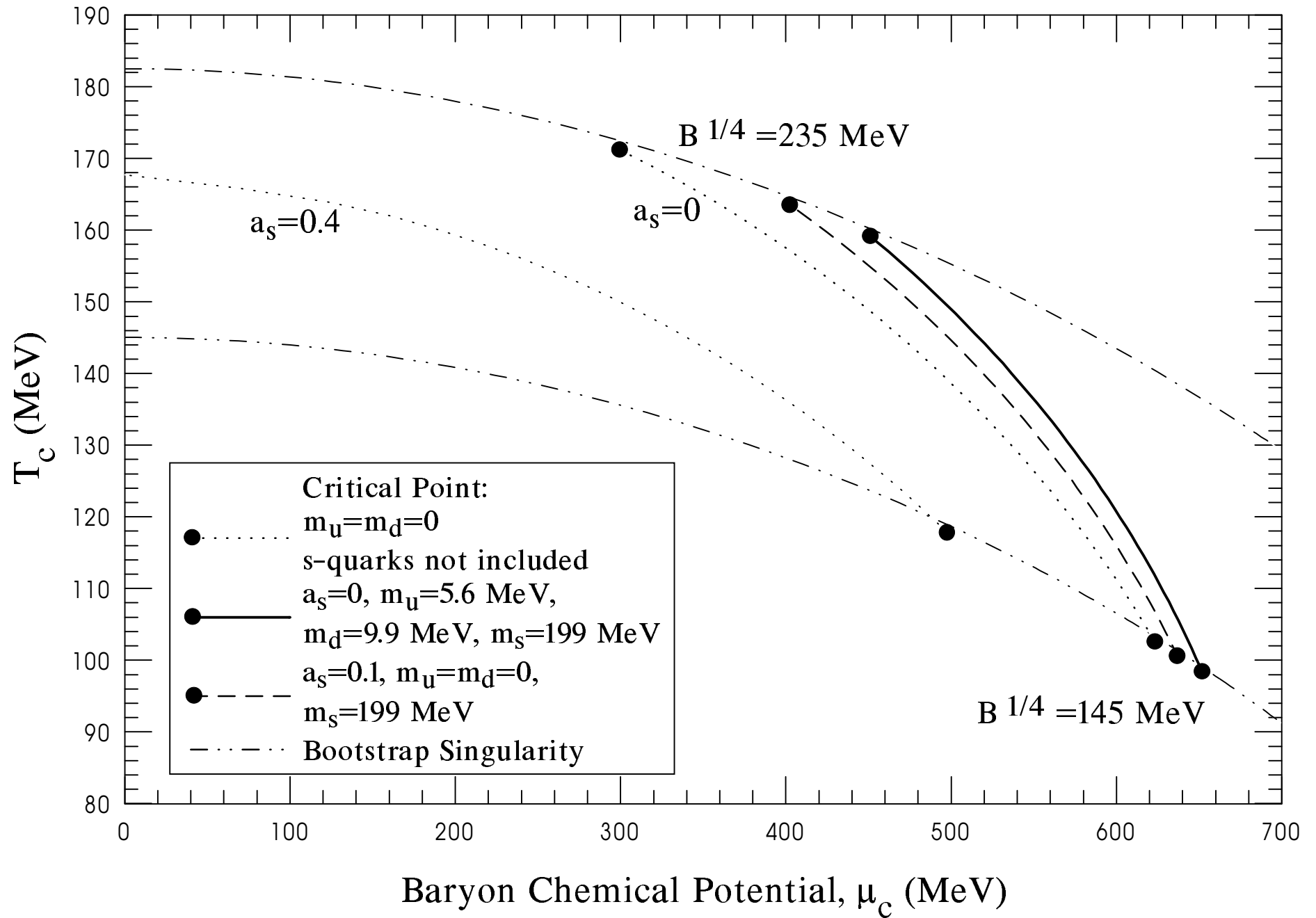


Fig. 6